CHAPTER 76

NUMERICAL MODEL INVESTIGATION OF SELECTED TIDAL INLET-BAY SYSTEM CHARACTERISTICS

William N. Seelig [1]
Robert M. Sorensen [2]

Abstract

A spatially integrated one-dimensional numerical model of inlet-bay hydraulics has been combined with a simple sediment transport model to investigate selected tidal inlet-bay system characteristics. A parametric study has been performed using the models to determine the effect of various factors on the net direction and order of magnitude of inlet channel flow and sediment transport. Factors considered include astronomical tide type, storm surge height and duration, variation in bay surface area, time-dependent channel friction factor, and the addition of a second inlet connecting the bay and sea.

Introduction

The purpose of this study is to investigate selected basic flow and sediment transport characteristics of tidal inlets. A simple numerical hydraulic-sediment transport model applied to an idealized inlet-bay system is used to evaluate the time-dependent channel ebb and flood flow velocity and sediment transport rate as well as the net and gross sediment transport rate for a tidal cycle. The independent variables investigated are:

1. Common tidal types found on the Atlantic, Gulf and Pacific coasts of the United States.
2. A normalized storm surge of varying peak height and duration.
3. A water-level dependent variable bay surface area.
4. Time-dependent channel resistance specified by a variable Manning coefficient.
5. A second inlet of varying cross-sectional area.

Inlet-Bay System

The idealized inlet shape used in this study (Figure 1) was designed to have characteristics typical of tidal inlets, but excludes

[1]Hydraulic Engineer, Coastal Structures Branch, US Army Coastal Engineering Research Center, Ft. Belvoir, Virginia 22060.

[2]Chief, Coastal Structures Branch, US Army Coastal Engineering Research Center, Ft. Belvoir, Virginia 22060

any ebb or flood tidal deltas. This idealized shape was developed during a classification study of many inlets throughout the United States.

The bay area is initially taken as independent of bay water level and the tidal wave length in the bay is assumed to be much longer than the longest axis of the bay.

Inlet Hydraulics

The numerical model of inlet hydraulics used in this study was reported earlier in Sorensen and Seelig (1976) and discussed in detail in Seelig et al. (1977). Important characteristics of the model are: (1) the continuity equation is used to relate rate of bay water level change, dh_b/dt to inlet velocity, V, by assuming that the surface water level is uniform throughout the bay at any time. That is

$$VA_c = A_b \frac{dh_b}{dt} \tag{1}$$

where A_b is the bay surface area and A_c is the inlet cross-sectional area. Storage of water in the inlet is neglected. (2) motion of water in the inlet is described by the one-dimensional equation of motion along the inlet channel axis:

$$-g \frac{d\eta}{dx} = \frac{fV|V|}{8R} + V\frac{dV}{dx} + \frac{dV}{dt} \tag{2}$$

where η is the water surface elevation, R is the channel hydraulic radius, x the distance along the channel axis from some reference point, f the channel friction factor, and g the acceleration of gravity. Eq. 2 relates the horizontal driving force due to the water surface slope to the channel frictional resistance, the convective acceleration caused by velocity variation along the channel axis, and the temporal acceleration (or inertia) caused by velocity variation with time.

In this numerical model the inlet is divided into a series of channels and cross-sections to produce a flow net grid. Each grid element is assigned a Manning's n, depth, width, and length. Eq. 2 is written in a finite element form. Equations (1) and (2) are then solved in a time marching procedure for solving differential equations with boundary conditions applied at each time step. Flow is assumed to follow the path of least resistance and the amount of flow in each grid element at each time step is determined accordingly.

This numerical model has been tested for a variety of inlets throughout the United States and found to be a reliable low-cost method for predicting the hydraulics of inlets.

The idealized inlet in Figure 1 was modeled using a semi-diurnal sinusoidal tide with an amplitude, a_o, of 61 cm and period, T, of 12.4 hours for various values of bay surface area. Figure 2 shows results of the hydraulic predictions where the phase lag and the dimensionless maximum velocity, V'_{max}, have been averaged for the flood and ebb portions

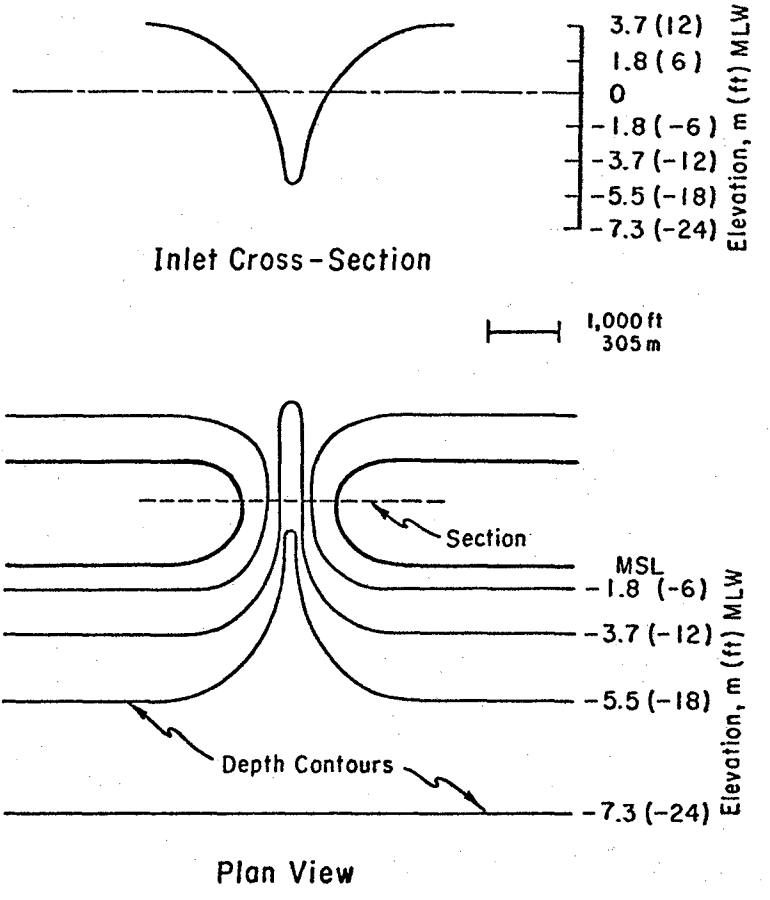

Figure 1. Idealized inlet

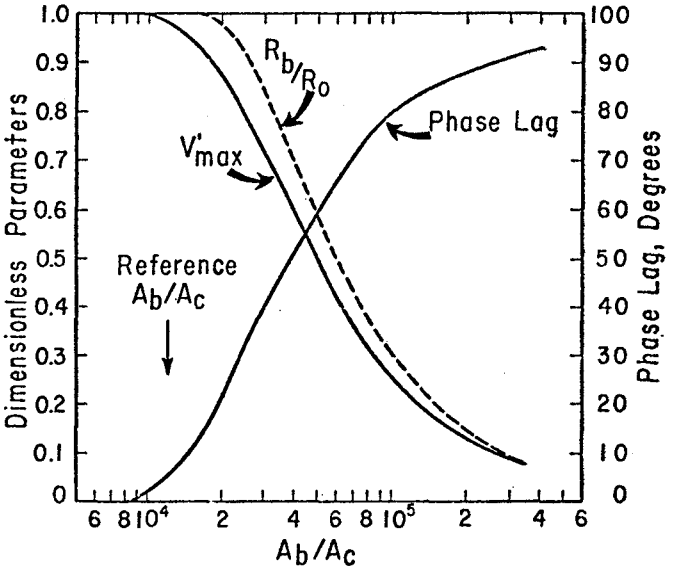

Figure 2. Inlet-bay hydraulic characteristics

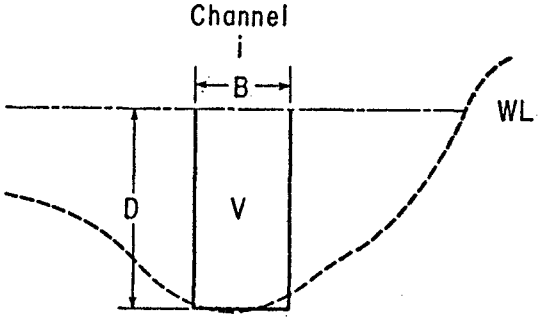

Sediment Transport

$$Q_s = k \sum_{\text{cross section}} B(|V|-V_c)^3 sg(V)$$

Figure 3. Sediment transport calculations

of the tidal cycle. We define

$$V'_{max} = V_{max} T A_c/(2\pi a_o A_b) \quad (3)$$

where V_{max} is the maximum channel velocity averaged across the throat cross section during a tidal cycle. Manning's n used in these calculations is taken as a weak function of channel water depth:

$$n = 0.038 - 0.0022 D \quad (4)$$

where D is the still water depth in meters for each grid.

Jarrett (1976) made a study of tidal inlets throughout the U.S. and presented a relationship between the cross-sectional area of the inlet at still water level and the tidal prism. This condition is satisfied for the idealized inlet where $A_b/A_c = 1.2 \times 10^4$. Conditions at this point are referred to as "the reference condition". For the reference condition the bay tide range is approximately equal to the tide range in the ocean.

Sediment Transport Model

The rate of sediment transport, Q_s, across the minimum cross-sectional area portion of the inlet is taken as:

$$Q_s = k \sum_{i=1}^{N} B(|V| - V_c)^3 \, sg\,(V) \quad (5)$$

where sg ( ) is the sign function, V is the velocity for a grid for a time step, $|V|$ is the magnitude of V, V_c is a critical velocity below which the sediment transport rate can be neglected (V_c is taken as 30 cm/sec in this study), N is the number of grid channels, and k is some unknown function influencing the transport rate (Figure 3) and B is the grid channel width. In this study k is taken as an unknown constant.

Figure 4 shows the predicted rate of sediment transport and average inlet throat velocity for the reference condition. Note that the maximum inlet velocity is slightly higher than 100 cm/sec, which is typical for natural tidal inlets. Changes in depth, cross-sectional flow area and frictional resistance throughout the tidal cycle produce asymmetries in water velocities that are magnified in the predicted rate of sediment transport. For example, the predicted rate of flood sediment transport for this case is higher but generally shorter in duration than for ebb.

The rate of sediment transport is integrated over the flood and ebb portions of the cycle to give volumes of transport, Q_f and Q_e. For the conditions in Figure 4 the flood transport is 20% higher than the ebb transport and the net transport volume is about one-tenth of the gross or total volume of sediment transport.

In the following sections, deviations from the reference conditions are systematically made and the predicted sediment transport volumes are compared to the reference condition.

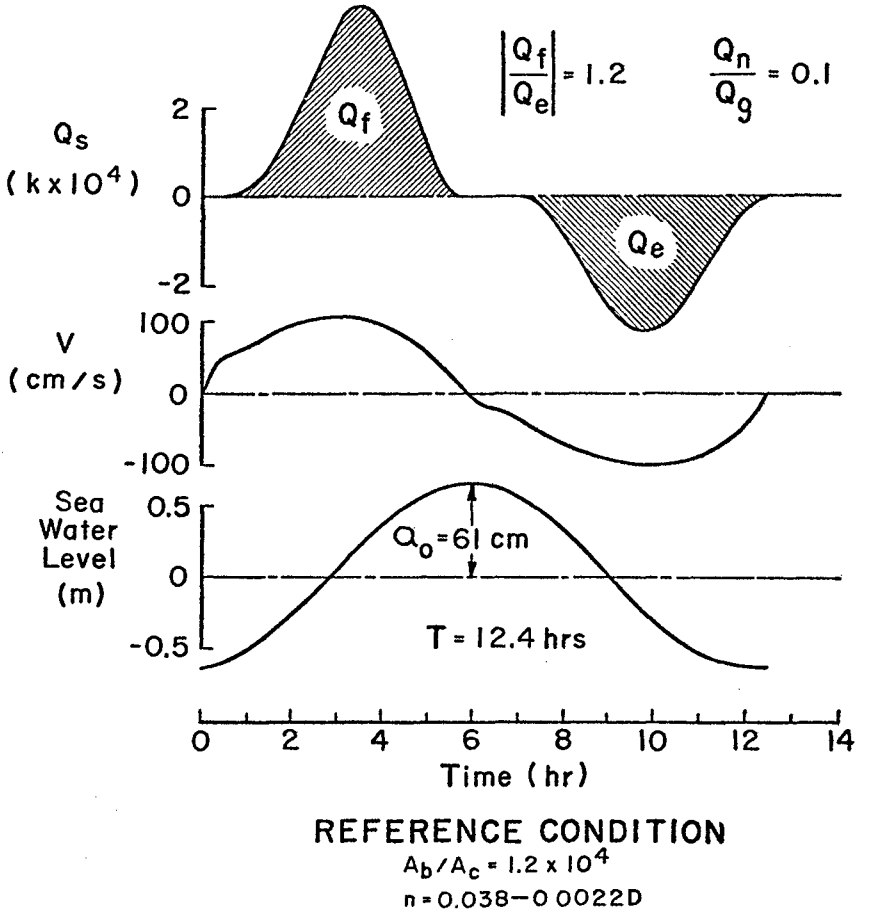

Figure 4. Hydraulic and sediment predictions for the reference condition

Influence of Tide Type

Astronomical tides are not strictly sinusoidal, as assumed in the reference condition, but are influenced by numerious astronomical and local affects. To obtain some idea of the effect of the astronomical tide type, tides were predicted for three locations (Wilmington, N.C., Galveston, Texas, and Los Angeles, California) using a computer program developed by D.L. Harris of CERC. Tides were predicted for the entire month of January 1981 and normalized by dividing by the root-mean-square of the water levels to give the tides the same energy. The relative amounts of calculated net and gross sediment transport and samples of the tide are given in Figure 5. These results suggest that for a fixed amount of tidal energy a semi-diurnal tide (top curve) produces the largest predicted gross transport with a relatively large net flood sediment transport, while a semi-diurnal tide with a strong inequality has lower gross transport and net transport in the ebb direction.

Storm surges investigated in this study are taken as having a normal shape with range in the ocean, R_o. The period of the surge is characterized by four times the standard deviation of the normal shape. Figure 6 illustrates a surge of this type and shows the predicted hydraulic response. The inlet velocities are highly asymmetrical due to inertia and non-linear effects.

Predicted sediment transport volumes for storm surges are given in Figure 7 for surges with durations of one to eight hours and various surge amplitudes. The left portion of the figure shows the ratio of predicted flood to ebb sediment transport. For most conditions investigated, the value of this ratio is greater than unity, indicating that more transport occurs on the flood than ebb portion of the tidal cycle. In the right section of the figure the gross amount of sediment transport is normalized by the gross transport predicted for the reference semi-diurnal tide condition. (The superscript (') indicates sediment transport has been normalized by conditions at the reference condition). The right portion of Figure 4 shows that the amount of transport during a surge can be an order of magnitude more than during astronomical tidal cycle.

The astronomical tide plus a storm surge produces a complicated pattern of sediment motion. The magnitude and direction of the sediment motion depends on the amplitude of the tide and are strongly influenced by the phase relation between the tide and surge. In conditions modeled, the gross transport for a surge plus tide reached as much as three times the value predicted for the surge and tide acting independently. Net transport was as high as one and one-half times larger.

Influence of Bay Surface Area

The bay surface area usually will not be constant with changing water level as was assumed in the reference condition. Flooding of tidal flats and sloping bay shores may dramatically change the bay surface area throughout the tidal cycle. A number of bay area variation models were tested and three are presented in this paper. First, bay area is assumed to be a linear function of bay level (Figure 8) and

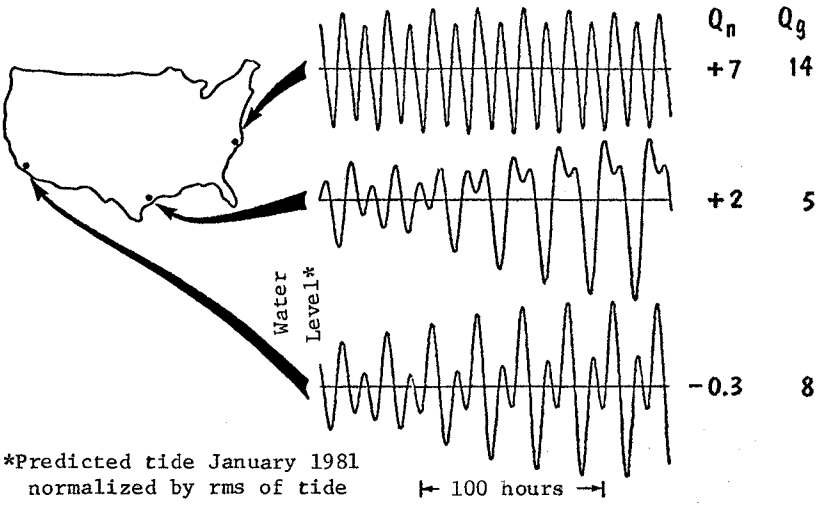

Figure 5. Incluence of tide type on sediment transport

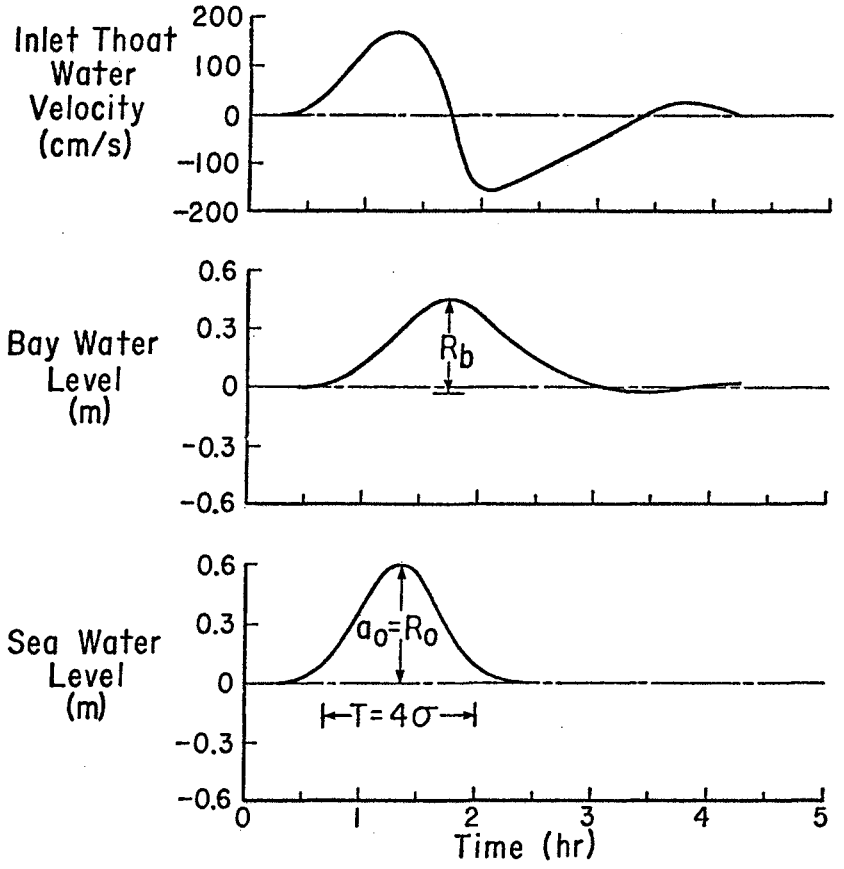

Figure 6. Inlet hydraulic response to a storm surge

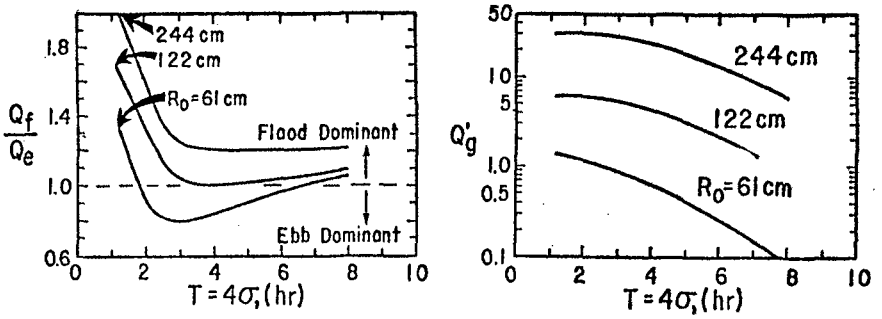

Figure 7. Sediment transport caused by a storm surge

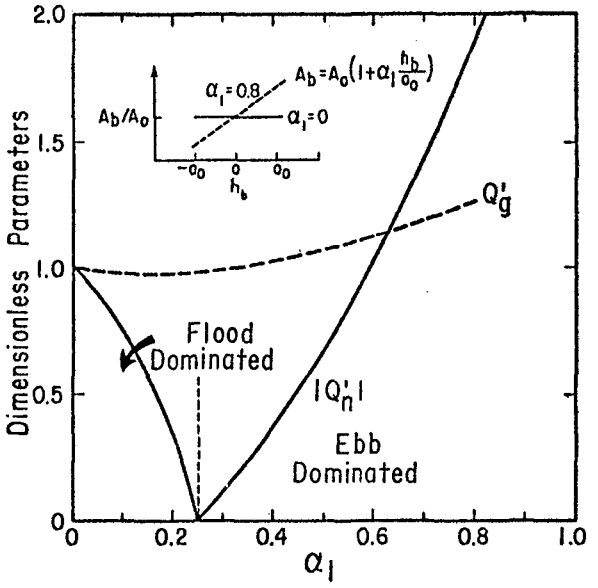

Figure 8. Effect of bay area variation on sediment transport

the amount of variation is characterized by the parameter, α_1. If $\alpha_1 = 0$, there is no bay surface area variation and the reference condition is reached. As α_1 increases larger variations occur in surface area as the water level changes (upper portion of the figure).

As the rate of surface area change is increased (α_1 gets larger) the amount of gross sediment transport increases while the tidal prism remains approximately constant. Less flood dominance is present, as shown by the net transport, so that for $\alpha_1 = 0.25$ there is no net sediment transport predicted. For $\alpha_1 > 0.25$ net transport is in the ebb direction.

As a second form of bay area variation the bay surface area below the still water level is taken as constant and there is a linear variation above the still water level (Figure 9). This case could correspond to a bay with extensive incised channels and well-developed tidal flats at or above the mean water level. The pattern of trends in sediment motion is similar for this bay area change model to that for the linear case. No net motion occurs when $\alpha_2 = 0.58$.

Results for an exponential bay area variation model are given in Figure 10. The transition between net flood and net ebb sediment transport for this bay area variation model occurs at $\alpha_3 = 0.28$.

Influence of Channel Resistance

In the reference condition the Manning's friction factor, n, was made to weakly decrease with channel depth (Equation 3). This encourages higher flow rates in deeper portions of the inlet channel, so that predicted gross sediment transport is higher than for a constant value of n (Figure 11). Higher values of n decrease gross transport, but actually increase the amount of net transport because asymmetries throughout the flow cycle are enhanced (Figure 11).

Behrens et al. (1977) carried out a field study on Corpus Christi Pass, a tidal inlet dominated by frictional effects. Manning's friction factor was computed for the inlet as a function of time and found to vary strongly throughout the tidal cycle. For most cases studied, n steadily increased until it reached a maximum towards the end of a ebb or flood portion of the tidal cycle. In some cycles the opposite pattern was observed. Both cases were investigated in the idealized inlet (Fig. 12).

The case of the increasing n is characterized by a velocity that rapidly changes at flow reversal and reaches a high value that is retained throughout much of the cycle. The situation where n decreases during the cycle has larger variation in velocity with time (Figure 12). Inspite of the differences in the shape of the velocity curves for these two cases, the gross and net amounts of predicted sediment transport are approximately the same. The volumes of sediment transport are approximately the same as if the mean value of n were used throughout the tidal cycle.

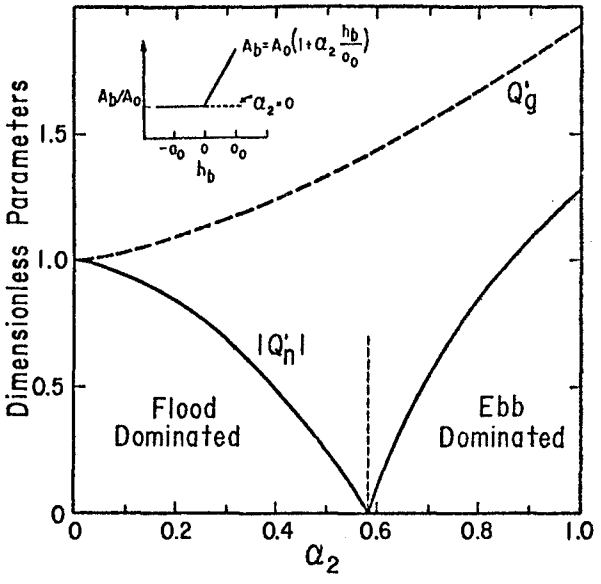

Figure 9. Effect of bay area variation on sediment transport

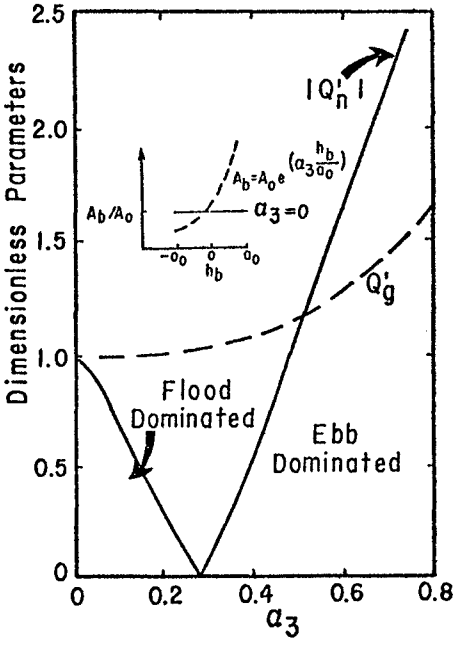

Figure 10. Effect of bay area variation on sediment transport

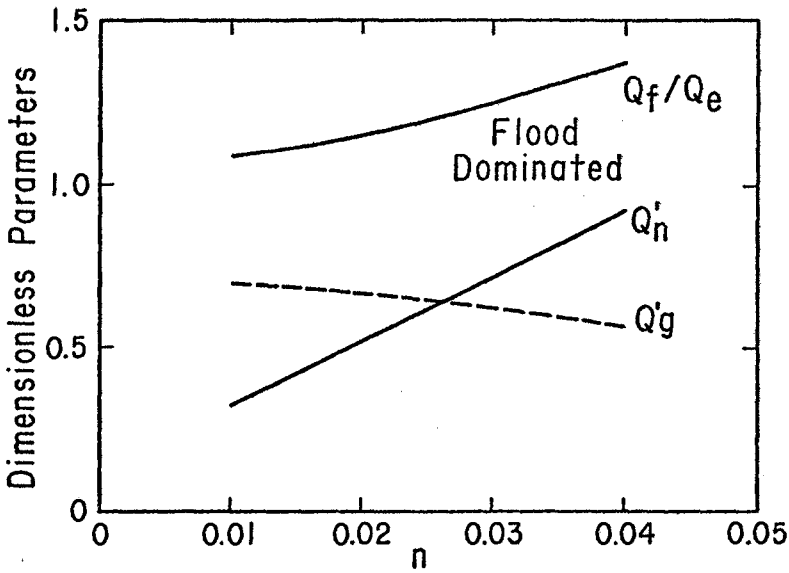

Figure 11. Effect of Manning's n on sediment transport

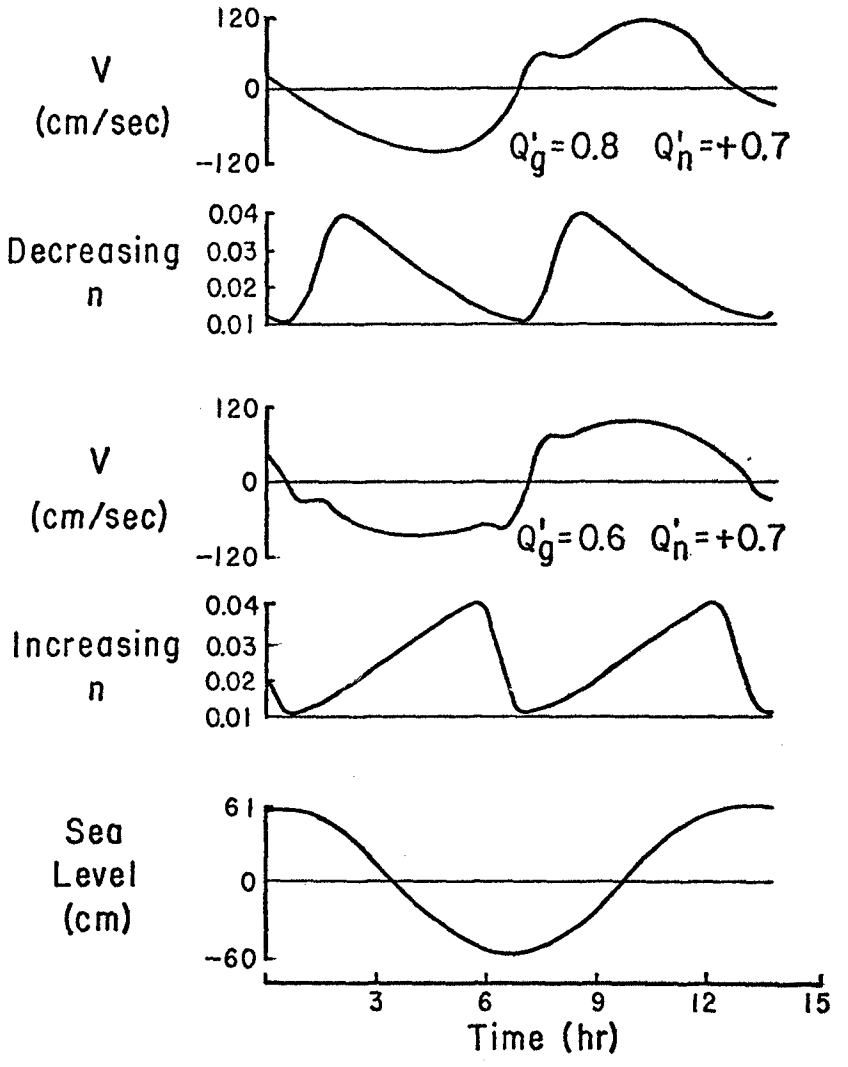

Figure 12. Effect of variable n on inlet hydraulics and sediment transport

Influence of a Second Inlet

A bay may be connected to an ocean by more than one inlet. The effect of a second inlet is examined by adding another inlet to the system with a length equal to the width of the barrier island. The second inlet is taken as prismatic with a width to depth ratio of 50, which was found as most typical for US inlets in an inlet classification study performed by Vincent (1978). Predicted transport volumes for the reference condition tide are shown in Figure 13.

As the size of the second inlet increases, the sediment transport in the idealized inlet rapidly decreases, so that when the cross-sectional areas are equal, $(A_{c1} + A_{c2})/A_{c1}=2$, the transport in the idealized inlet is less than ten percent of that at the reference condition. Total transport in the second inlet increases as its area increases until transport reaches a maximum when the cross-sectional area is approximately half of the idealized inlet. The sediment transport in the idealized inlet is generally larger than in the second inlet because the idealized inlet's deep gorge makes it more hydraulically efficient.

Summary and Conclusions

A numerical model investigation of the sediment transport in a realistic inlet shape shows that:

(1) A semi-diurnal tide produces the largest amount of sediment motion and gives a net flood sediment transport, when several tides types of equal energy are compared.

(2) Storm surges can move significantly more sediment than is moved during an astronomical tidal cycle. The phasing of a surge and tide is especially important in determining the amount and net direction of transport.

(3) If the surface of the bay changes as the bay water level fluctuates there will tend to be less flood sediment motion and more ebb sediment motion than for the case of no bay area change.

(4) High inlet friction enhances flow asymmetries so net sediment transport increases while gross sediment transport decreases. An inlet with a Manning's n friction factor that varies throughout the cycle produces approximately the same amount of sediment transport as the inlet with the mean value of n.

(5) A second inlet may greatly reduce the amount of sediment transport in the primary inlet and the total transport of the two inlets can be smaller than if only the first inlet connects the bay and ocean.

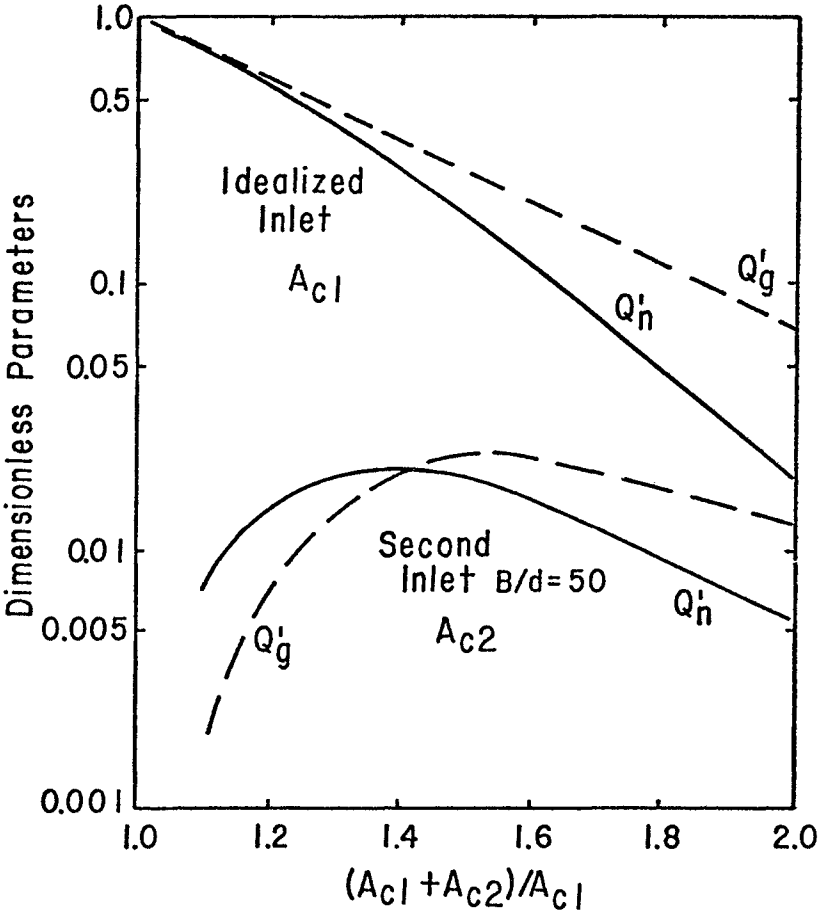

Figure 13. Effect of a second inlet on sediment transport

Acknowledgment

The analysis and results presented in this paper, unless otherwise noted, were based on research conducted at the Coastal Engineering Research Center under the Coastal Engineering Research Program of the U.S. Army Corps of Engineers. The findings of this paper are not to be construed as official Department of the Army position unless so designated by other authorized documents. Permission to publish this information is appreciated.

REFERENCES CITED

Behrens, E. W., Watson, R. L. and Mason, C., "Hydraulics and Dynamics of New Corpus Christi Pass, Texas: A Case History, 1972-73", GITI Report No. 8, CERC-WES, January 1977.

Jarrett, J. T., "Tidal Prism - Inlet Area Relationships", CERC-WES General Investigation of Tidal Inlets Report 3, February 1976.

King, D. B., and Shemdin, O. H., "Modeling of Inlet-Bay Systems in Relation to Sand Trapping", Symposium of the Waterways, Harbors and Coastal Engineering Division, ASCE, 1975, pp 1623-1637.

Seelig, W., "Computer Program Documentation - INLET2", unpublished report, U.S. Army Coastal Engineering Research Center, Ft. Belvoir, VA. 13 December 1976.

Seelig, W., Harris, D. L. and Herchenroder, B. E., "A Spatially Integrated Numerical Model of Inlet Hydraulics", CERC-WES General Investigation of Tidal Inlets Report 14, November 1977.

Sorensen, R. M. and Seelig, W., "Hydraulics of Great Lakes Inlet - Harbors Systems", Proceedings Fifteenth Coastal Engineering Conference, ASCE, July 1976, pp. 1646-1665.

Vincent, L., "The Geometry of Selected Tidal Inlets", CERC-WES General Investigation of Tidal Inlets Report (in publication), U.S. Army Coastal Engineering Research Center, Ft. Belvoir, VA 22060, 1978.

SYMBOLS

A_b	bay surface area
A_b'	dimensionless bay surface area = A_b/A_c
A_b^*	reference bay surface area
A_c	inlet cross-sectional area at the throat
A_o	bay surface area at the still water level
a_o	sea tidal or surge amplitude
B	inlet grid width
d	water depth
f	channel friction factor
g	acceleration of gravity
h_b	bay water level
k	sediment transport factor (value unknown)
n	Manning's bottom friction coefficient
P	tidal prism
Q_e	ebb sediment transport
Q_f	flood sediment transport
Q_g'	dimensionless gross sediment transport normalized by the reference condition
Q_g^*	reference gross sediment transport
Q_n'	dimensionless net sediment transport normalized by the reference condition
Q_n^*	reference net sediment transport
Q_s	rate of sediment transport
R	hydraulic radius
R_b	bay tidal range
R_o	sea tidal range
t	time
V	instaneous flow velocity
V_c	threshold velocity for sediment motion
V_{max}	maximum inlet velocity at the inlet throat (mean of ebb and flood for periodic flow)
V_{max}'	dimensionless maximum inlet velocity
X	distance
α_1, α_2, α_3	bay surface area variation parameters
η	water level